# IceBridge Snow Radar L1B Geolocated Radar Echo Strength Profiles, Version 1

## USER GUIDE

**How to Cite These Data**

As a condition of using these data, you must include a citation:

Paden, J., J. Li, C. Leuschen, F. Rodriguez-Morales, and R. Hale. 2010, updated 2016. *IceBridge Snow Radar L1B Geolocated Radar Echo Strength Profiles, Version 1*. [Indicate subset used]. Boulder, Colorado USA. NASA National Snow and Ice Data Center Distributed Active Archive Center. doi: https://doi.org/10.5067/05LF3JANL51I. [Date Accessed].

National Snow and Ice Data Center

# TABLE OF CONTENTS

# 1   DATA DESCRIPTION

The Snow Radar L1B Geolocated Radar Echo Strength Profiles data set includes echograms with measurements for time, latitude, longitude, elevation, as well as flight path charts and echogram images.

## 1.1 File Information

### 1.1.1   Format

The binary files contain a vector stream of record data. Each record includes seven header values and a Fast Fourier Transform (FFT) window of snow radar data. The FFT window has dimensions N-number of range bins.

The digital image files are JPEG files. The y-axis in the FFT JPEG files shows depth relative to a range around the surface. The surface is in the center of the y-axis and the y-axis is set to a fixed range, usually from 0 m to 60 or 80 m for the land ice, and 0 m to 4 m for sea ice.

The MATLAB files are binary files produced and readable by the proprietary Matlab software or other tools such as the Octave high-level language.

The KML files are flight line browse images for each segment.

The most convenient way to browse the imagery quickly is through the JPEG files. The quickest way to plot the data set is to look at the KML browse files for the entire season.

#### 1.1.1.1  2011 Antarctica Data

The 2011 Antarctica MATLAB data are divided into segments. A segment is a contiguous data set where the radar settings do not change. A day is divided into segments if the radar settings were changed, hard drives were switched, or other operational constraints required that the radar recording be turned off and on. All data from a particular segment are stored in a directory with the following nomenclature YYYYMMDD_SS where YYYY is the year, MM is the month, DD is the day, and SS is the segment. Segments are always sorted in the order in which the data were collected. Currently at NSIDC, the data directories for 2011 Antarctica are named according to this convention, but the previous year directories are not.

Each segment is broken into frames, analogous to satellite SAR scenes, to make analyzing the data easier. Frames span 33 seconds covering 4 to 5 km dependent upon aircraft speed. The

frame ID is a concatenation of the segment ID and a frame number and follows the format YYYYMMDD_SS_FFF where FFF is the frame number from 000 to 999. Generally the FFF starts with 0 or 1 and increments by 1 for each new frame, but this is not always the case; only the ordering is guaranteed to match the order of data collection.

For each data frame there is a flight path file (0map) and an echogram file (1echo).

## 1.1.2   Naming Convention

### 1.1.2.1  Binary Files

The binary files are named according to the following convention and as described in Table 1:

data01.0180.bin
dataSS.xxxx.bin

Table 1. Binary File Naming Convention

| Variable | Description |
|----------|-------------|
| data | Indicates data file |
| SS | Day segment |
| xxxx | Flight ID number |
| .bin | Indicates a binary file |

### 1.1.2.2  MATLAB Files

The MATLAB files for 2011 Antarctica are named according to the following convention and as described in Table 2:

Data_20110316_01_000.mat
Data_YYYYMMDD_SS_FFF.mat

Table 2. MATLAB File Naming Convention

| Variable | Description |
|----------|-------------|
| Data | Indicates data file |
| YYYY | Four-digit year |
| MM | Two-digit month |
| DD | Two-digit day |
| SS | Day segment |
| FFF | Frame number |
| .mat | Indicates a MATLAB file |

The flight track MATLAB files and GPS MATLAB files are named according to the following convention and as described in Table 3.

flight_track.mat
gps.mat

Table 3. Flight Track and GPS MATLAB File Naming Convention

| Variable | Description |
|---|---|
| flight_track or gps | Indicates flight track file or GPS file |
| .mat | Indicates MATLAB file |

## 1.1.2.3  JPEG Files

The FFT image JPEG files and Flight Path image JPEG files are named according to the following convention and as described in Table 4.

FFT_image.00.0001.jpg
FFT_image.SS.xxxx.jpg
Flight_Path.00.0001.jpg
Flight_Path.SS.xxxx.jpg

Table 4. FFT Image JPEG and Flight Path Image JPEG File Naming Convention

| Variable | Description |
|---|---|
| FFT_image or Flight_Path | FFT_image = echogram browse image<br>Flight_Path = flight path location plot |
| SS | Day segment |
| xxxx | Flight ID number |
| .jpg | Indicates JPEG image file |

The flight track image JPEG files are named according to the following convention and as described in Table 5.

flight_track_image10162009.jpg
flight_track_imageMMDDYYYY.jpg

Table 5. Flight Track Image JPEG File Naming Convention

| Variable | Description |
|---|---|
| flight_track_image | Flight track image map |
| MM | Two-digit month |
| DD | Two-digit day |
| YYYY | Four-digit year |
| .jpg | Indicates JPEG image file |

For each data frame of the 2011 data, there is a flight path file (0map) and an echogram file (1echo). The file naming conventions are shown below and as described in Table 6.

20110316_01_000_124503_0maps.jpg
20110316_01_000_124503_1echo.jpg
YYYYMMDD_SS_FFF_HHmmss_0maps.jpg
YYYYMMDD_SS_FFF_HHmmss_1echo.jpg

Table 6. Flight Path and Echogram File Naming Variables

| Variable | Description |
|----------|-------------|
| YYYY | Four-digit year |
| MM | Two-digit month |
| DD | Two-digit day |
| SS | Segment number |
| FFF | Frame number |
| HHmmss | GPS time stamp for the first range line in the image where HH is 00-23 hours, mm is 00-59 minutes, and ss is 00-59 seconds. |
| 0maps | Flight path file |
| 1echo | Echogram file |
| .jpg | Indicates JPEG image file |

### 1.1.2.4  KML Files

The KML browse image files, for 2011 Antarctica only, are named according to the following convention and as described in Table 7.

Browse_Data_20111012_01.kml
Browse_Data_YYYYMMDD_SS.kml

Table 7. KML Browse Image File Naming Convention

| Variable | Description |
|----------|-------------|
| Browse_Data | Indicates browse data file |
| YYYY | Four-digit year |
| MM | Two-digit month |
| DD | Two-digit day |
| SS | Day segment |
| .kml | Indicates KML file |

## 1.2 Volume

The entire data set is approximately 1.15 TB.

## 1.3 Spatial Information

### 1.3.1 Coverage

Spatial coverage for the IceBridge snow radar campaigns include the Antarctica and surrounding ocean areas. In effect, this represents the coverage noted below.

Antarctica:

Southernmost Latitude: 90° S

Northernmost Latitude: 53° S

Westernmost Longitude: 180° W

Easternmost Longitude: 180° E

### 1.3.2 Resolution

Spatial Resolution varies dependent on along-track, cross-track, and aircraft height characteristics.

### 1.3.3 Geolocation

Referenced to WGS-84 Ellipsoid.

## 1.4 Temporal Information

### 1.4.1 Coverage

These data were collected as part of Operation IceBridge funded campaigns from 16 October 2009 to 19 November 2011.

### 1.4.2 Resolution

IceBridge campaigns are conducted on an annual repeating basis. Arctic and Greenland campaigns are conducted during March, April, and May, and Antarctic campaigns are conducted during October and November.

## 1.5 Parameter or Variable

The Snow Radar L1B Geolocated Radar Echo Strength Profiles data set contains radar backscatter measurements sensitive to snow thickness and internal layering, collected over land ice and sea ice.

## 1.5.1 The Snow Radar MATLAB files contain fields as described in Table 8.

Table 8. MATLAB File Parameter Description

| Parameter | Description | Units |
|---|---|---|
| Data | Radar echogram data. The data may be truncated. Presence of the Truncate_Bins variable indicates data has been truncated. Lack of the Truncate_Bins variable indicates data has not been truncated. | Represents relative received power (Watts) |
| Time | Fast time. Zero time is approximately the beginning of the transmit event. | Seconds |
| Depth | Range axis with the origin at the median of the Surface values in this frame and assuming a dielectric of 1.53 (Depth = (Time - median(Surface)) * c/2/sqrt(1.53)) | Meters |
| Truncate_Bins | Indices into the Time and Depth vectors for which the Data is available. Only available when Data are truncated. | n/a |
| Truncate_Mean | Represents a mean of the noise power for the truncated range bins before the surface return. When no range bins were truncated before the surface return the value is NaN. Only available when Data are truncated. | n/a |
| Truncate_Median | Represents a median of the noise power for the truncated range bins before the surface return. When no range bins were truncated before the surface return the value is NaN. Only available when Data are truncated. | n/a |
| Truncate_Std_Dev | Represents a standard deviation of the noise power for the truncated range bins before the surface return. When no range bins were truncated before the surface return the value is NaN. Only available when Data are truncated. | n/a |
| GPS_Time | GPS time when data were collected, seconds since January 1, 1970 00:00:00. This is the ANSI C standard. | Seconds |
| Latitude | WGS-84 geodetic latitude coordinate where data were collected, potentially modified by motion compensation. Always referenced to North. Represents the location of the origin of the trajectory data which is generally not the radar's phase center, but some other point on the aircraft, for example the GPS antenna or the INS. | Degrees |

| Parameter | Description | Units |
|---|---|---|
| Longitude | WGS-84 geodetic longitude coordinate where data were collected, potentially modified by motion compensation. Always referenced to East. Represents the location of the origin of the trajectory data which is generally not the radar's phase center, but some other point on the aircraft, for example the GPS antenna or the INS. | Degrees |
| Elevation | Elevation where data were collected, potentially modified by motion compensation. Referenced to WGS-84 ellipsoid. Positive is outward from the center of the Earth. Represents the location of the origin of the trajectory data which is generally not the radar's phase center, but some other point on the aircraft, for example the GPS antenna or the INS. | Meters |
| Elevation_Correction | Represents the number of zeros that were inserted during elevation compensation for each range line to simulate near-level flight. These zeros are not included in the truncation noise statistics. Only available when data are elevation compensated. | Range bins |
| Surface | Estimated two way propagation time to the surface from the collection platform. This uses the same frame of reference as the Time variable. This information is sometimes used during truncation to determine the range bins that can be truncated. | Seconds |
| *param* | Multiple variables with a name containing the string "param." Contains radar and processing settings, and processing software version and time stamp information. Fields of structures are not static and may change from one version to the next. | |

# 2 DATA ACQUISITION AND PROCESSING

## 2.1 Acquisition

The CReSIS snow and ku-band radars use a Frequency Modulated Continuous Wave (FMCW) architecture (Carrara et al. 1995). This is done to reduce the required sampling frequency of the Analog to Digital Converter (ADC) and is possible when the range gate is limited. Currently, the range gate is limited to low altitude flights. In the FMCW radars, a long, approximately 250 µs, chirp signal is generated which sweeps linearly in frequency from the start frequency to the stop frequency. This signal is transmitted and also fed to a mixer in the receiver to be used to demodulate the received signal. Signals outside the range gate are suppressed and aliased by the system.

The dominant scattered signal is the specular or coherent reflection from the air-snow surface and shallow layers beneath the surface. A bistatic antenna configuration is used to provide isolation between the transmit and receive paths which is important because the FMCW system receives while transmitting and too little isolation means that the direct path from the transmitter to the receiver will be too strong and will saturate the receiver. The antennas are mounted so the main beam is pointed in the nadir direction to capture the specular surface and layer reflections.

The Pulse Repetition Frequency (PRF), or along-track sampling rate, does not necessarily capture the full Doppler bandwidth for point scatterers without aliasing. However, since the target energy is mostly coherent, it occupies only a small portion of the Doppler spectrum so the undersampling in along-track is not generally a problem. Since the coherent portion of the surface and layer scattering is the primary signal of interest, presumming is used to lower the data rate which effectively low-pass-filters and decimates the Doppler spectrum.

## 2.2 Derivation Techniques and Algorithms

Echograms posted include altitude correction, but the binary files do not. Correction can be applied by shifting a record from bottom to top by the altitude correction value. Altitude variations within a data file are removed by subtracting the minimum altitude from all values. The result is variation in meters from the minimum. These values are then converted to whole pixel values given the radar parameters: sampling frequency = 58.32 MHz, pulse duration, FFT length, and bandwidth. Sampling frequency after the 2009 Greenland campaign is 62.5 MHz.

The code below shows how to load the data in Matlab to generate typical figures, and the illustrations show examples of the figures that were generated from the code.

```
snow = load('Data_20110316_03_035.mat');

figure(1); clf;
imagesc([],snow.Depth(snow.Truncate_Bins),10*log10(snow.Data));
colormap(1-gray(256));
xlabel('Range line');
ylabel('Depth (m)');
hc = colorbar;
set(get(hc,'ylabel'),'string','Relative power (dB)');

figure(2); clf;
imagesc([],1e6*snow.Time(snow.Truncate_Bins),10*log10(snow.Data));
hold on;
plot(1e6*snow.Surface);
hold off;
colormap(1-gray(256));
xlabel('Range line');
ylabel('Time (us)');
hc = colorbar;
set(get(hc,'ylabel'),'string','Relative power (dB)');

figure(3); clf;
h1 = plot(snow.Truncate_Mean);
hold on;
h2 = plot(snow.Truncate_Median,'r');
h3 = plot(snow.Truncate_Std_Dev,'g');
hold off;
xlabel('Range line');
ylabel('Power');
title('Truncated bins noise statistics');
legend([h1 h2 h3], 'Mean', 'Median', 'Std Dev');

% To reconstruct original data as closely as possible
Data = zeros(length(Time),size(snow.Data,2));
Data(snow.Truncate_Bins,:) = snow.Data;
c = 2.997924580003452e+08;
dt = snow.Time(2)-snow.Time(1);
dr = dt * c/2;
for rline = 1:size(Data,2)
   Data(:,rline) = circshift(Data(:,rline),-snow.Elevation_Correction(rline));
   snow.Elevation(rline) = snow.Elevation(rline) - snow.Elevation_Correction(rline)*dr;
   snow.Surface(rline) = snow.Surface(rline) - snow.Elevation_Correction(rline)*dt;
end
figure(4); clf;
imagesc([],snow.Time,10*log10(Data));
hold on;
plot(snow.Surface);
hold off;
colormap(1-gray(256));
xlabel('Range line');
ylabel('Range bin');
hc = colorbar;
set(get(hc,'ylabel'),'string','Relative power (dB)');
```
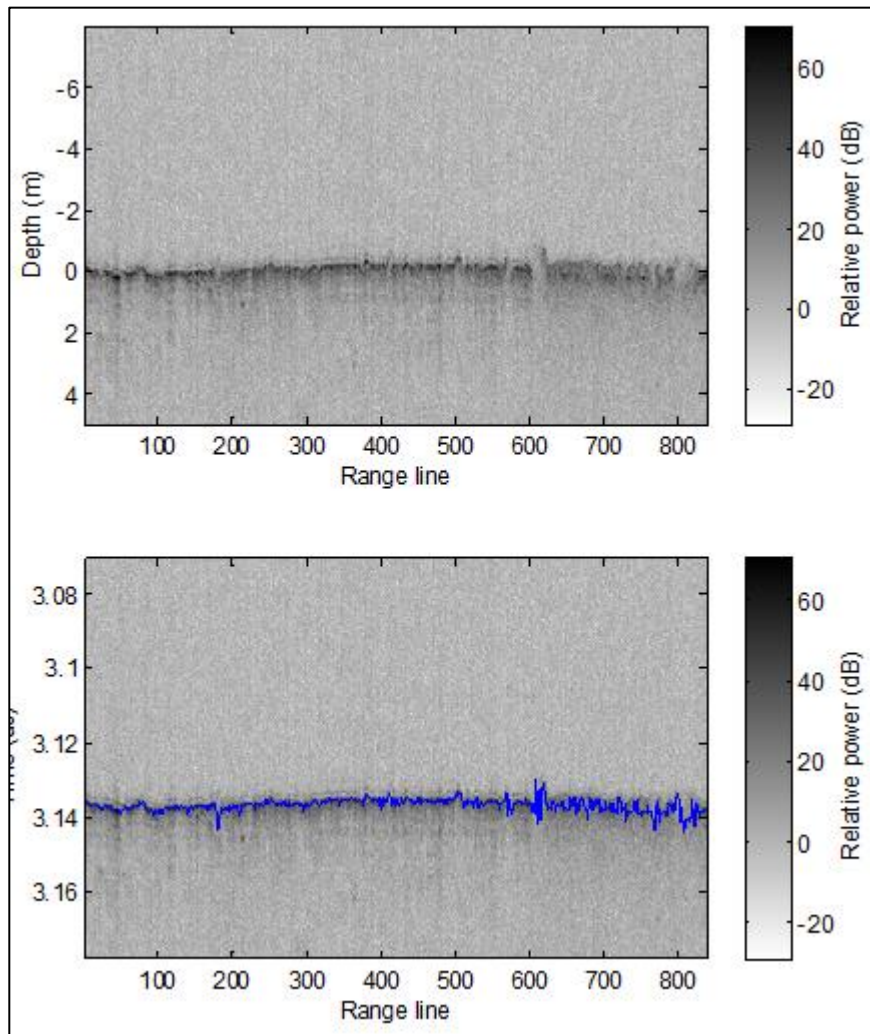
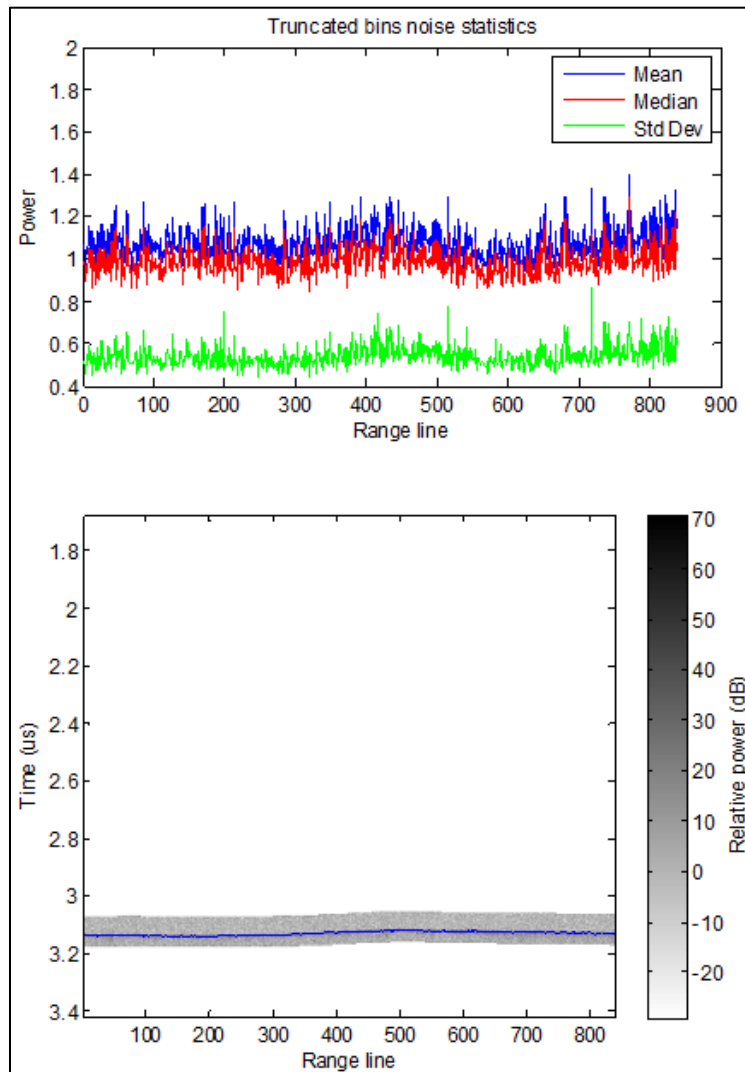Figure 1. Sample data.

Figure 2. Relative Power

Figure 3. Data samples of relative power.

## 2.3 Resolution and Error Bounds

### 2.3.1 Flat Surface Range Resolution

For a flat surface the range resolution is expressed by Equation 1:

$$\frac{k_t c}{2Bn}$$ **(Equation 1)**

Table 9. Flat Surface Range Resolution

| Variable | Description |
|---|---|
| $k_t$ | $k_t$ = 1.6 due to the application of a Hanning time-domain window to reduce the range sidelobes of the chirped transmit waveform |
| $c$ | Speed of light in a vacuum |
| B | Bandwidth, nominally 4500 MHz (2 to 6.5 GHz range) |
| n | Index of refraction for the medium |

## 2.3.2   Bandwidth

The bandwidth for a particular segment can be determined by reading the param_radar structure in the echogram data file or by looking at the parameter spreadsheet values f0, f1, and fmult and doing the calculation in Equation 2:

**(Equation 2)**

$$B = (param\_radar.f1 - param\_radar.f0) * param\_radar.fmult$$

Table 10. Segment Bandwidth

| Variable | Description |
|---|---|
| B | Bandwidth |
| param_radar.f1 | Stop frequency of chirp out of Direct Digital Synthesis (DDS) and into Phase-Locked Loop (PLL) |
| param_radar.f0 | Start frequency of chirp out of DDS and into PLL |
| param_radar.fmult | PLL frequency multiplication factor |

The range resolutions for several indices of refraction are shown in Table 12.

Table 11. Range Resolutions

| Index of Refraction | Range Resolution (cm) | Medium |
|---|---|---|
| 1 | 5.0 | Air |
| sqrt(1.53) | 4.0 | Snow |
| sqrt(3.15) | 2.8 | Solid Ice |

## 2.3.3   Index of Refraction

The index of refraction can be approximated by Equation 3:

$$n = \left(1 + 0.51\rho_{snow}\right)^3 \quad \textbf{(Equation 3)}$$

Table 12. Index of Refraction

| Variable | Description |
|----------|-------------|
| ρsnow | Density of the snow in grams per cm3 |

In the data, a dielectric of 1.53 is used which corresponds to a snow density of 0.3 g per cm$^3$ (Warren 1999).

## 2.3.4 Along-Track Resolution

In the along-track dimension, the raw data before any hardware or software coherent averages have a resolution derived in the same manner as the cross-track resolution. However, a basic form of focusing is applied called unfocussed Synthetic Aperture Radar (SAR) processing, also known as stacking or coherent averaging. If all affects are accounted for, the data may be coherently averaged to the SAR aperture length defined by Equation 4.

$$L = \sqrt{\frac{H\lambda_c}{2}} \quad \textbf{(Equation 4)}$$

Table 13. SAR Aperture Length

| Variable | Description |
|----------|-------------|
| H | Height above ground level |
| $\lambda_c$ | Wavelength at the center frequency |

For $H = 500$ m, data may be averaged to a length of 4.3 m. The resolution turns out to be approximately equal to this with the actual resolution definition given below. However, these data are only coherently averaged 16 times which includes both hardware and software averaging, and decimated by this same amount. At a platform speed of 140 m/s this is an aperture length, $L$, of 1.12 m. The sample spacing is likewise 1.12 m. The actual resolution is substantially less fine. The approximation is given by Equation 5.

$$\sigma_{x,SAR-qlook} = H \tan\left(\sin^{-1}\left(\frac{\lambda_c}{2L}\right)\right) \quad \textbf{(Equation 5)}$$

Table 14. Actual Resolution

| Variable | Description |
|----------|-------------|
| H | Height above ground level |

| Variable | Description |
|---|---|
| $\lambda_c$ | Wavelength at the center frequency |
| L | Aperture length |

For H = 500 m, the along-track resolution is 16.7 m.

A 1 range-bin by 5 along-track-range-line boxcar filter is applied to the power detected data and then decimated in the along-track by 5 so the data product has an along-track sample spacing of 5.6 m.

## 2.3.5   Fresnel Zone and Cross Track Resolution

For a smooth or quasi-specular target, for example internal layers, the primary response is from the first Fresnel zone. Therefore, the directivity of specular targets effectively creates the appearance of a cross-track resolution equal to this first Fresnel zone. The first Fresnel zone is a circle with diameter given by Equation 6.

$$\sigma_{y,\text{Fresnel}-\text{limited}} = \sqrt{2\left(H + T/\sqrt{3.15}\right)\lambda_c} \qquad \textbf{(Equation 6)}$$

Table 15. First Fresnel Zone Diameter

| Variable | Description |
|---|---|
| H | Height above the air/ice interface |
| T | Depth in ice of the target |
| $\lambda_c$ | Wavelength at the center frequency |

Table 16 gives the cross-track resolution for this case.

Table 16. Cross-track Resolution Case

| Center Frequency (MHz) | Cross-track Resolution H = 500 m T = 0 m |
|---|---|
| 3500 | 8.7 |

For a rough surface with no appreciable layover, the cross-track resolution will be constrained by the pulse-limited footprint, approximated in Equation 7.

$$\sigma_{y,\text{pulse}-\text{limited}} = 2\sqrt{\frac{\left(H + T/\sqrt{3.15}\right)ck_t}{B}} \qquad \textbf{(Equation 7)}$$

Table 17. Pulse-Limited Footprint

| Variable | Description |
|---|---|
| H | Height above the air/ice interface |
| T | Depth in ice of the target |
| c | Speed of light in a vacuum |
| $k_t$ | $k_t$ = 1.5 due to the application of a hanning time-domain window to reduce the range sidelobes of the chirped transmit waveform |
| B | Bandwidth in radians |

Table 18 gives the cross-track resolution with windowing.

Table 18. Cross-track Resolution with Windowing

| Bandwidth (MHz) | Cross-track Resolution H = 500 m T = 0 m |
|---|---|
| 4500 | 14.1 |

## 2.3.6   Footprint

The antenna installed in the bomb bay of the P-3 aircraft and the wing roots of the DC-8 aircraft is an ETS Lindgren 3115. The E-plane of the antenna is aligned in the along-track for the P-3 and in the cross-track for the DC-8. The approximate beamwidths are 45 degrees in along-track and 45 degrees in cross-track. The footprint is a function of range as shown in Equation 8.

$$\sigma = 2H \tan\left(\frac{\beta}{2}\right)$$   **(Equation 8)**

Table 19. Footprint

| Variable | Description |
|---|---|
| H | Height above ground level. For H = 500 m, the footprint is 414 m in along-track and 414 m in cross-track. |
| β | Beamwidth in radians |

## 2.3.7   Trajectory and Attitude Data

The trajectory data used for this data release was from a basic GPS receiver. Lever arm and attitude compensation has not been applied to the data.

## 2.3.8   Processing Steps

The following processing steps are performed by the data provider.

1. Set digital errors to zero. Error sequences are 4 samples in length and occur once every few thousand range lines.
2. Synchronization of GPS data with the radar data using the Universal Time Code (UTC) time stored in the radar data files.
3. Conversion from quantization to voltage at the ADC input.
4. Removal of DC-bias by subtracting the mean.
5. The quick look output is generated using presumming or unfocused SAR processing for a total of 16 coherent averages which includes hardware and software averages. If the PRF is 2000 Hz, the new effective PRF is 125 Hz.
6. A fast-time FFT is applied with a Hanning window to convert the raw data into the range domain, analogous to pulse compression. The data are flipped around based on the Nyquist zone.
7. A high pass filter is applied in the along-track to remove coherent noise.
8. A 1 range-bin by 5 along-track-range-line boxcar filter is applied to the power detected data and then decimated in along-track by 5.
9. The quick look output is used to find the ice surface location, fully automated.
10. The output is elevation compensated with radar range bin accuracy and then truncated in fast time based on the data posting settings in the parameter spreadsheet.

The purpose of the elevation compensation, when applied, is to remove the large platform elevation changes to make truncation more effective. The process is not designed to perform precision elevation compensation and is probably not sufficient for scientific analysis. The following steps are performed.

1. Let:
   A. Elevation_Orig be the 1 by N elevation vector before elevation compensation.
   B. Data_Orig be the M_orig by N data matrix before elevation compensation.
   C. Time_Orig be the M_orig by 1 fast-time time axis before elevation compensation.
   D. Elevation be the 1 by N vector from the data product file.
   E. Data be the matrix from the data product file.
   F. Time be the M by 1 fast-time time axis from the data product file maxElev = max(Elevation_Original).
2. dRange = maxElev − Elevation_Original
3. dt = Time_Orig(2) − Time_Orig (1)
   A. Sample spacing in fast-time (i.e. one range bin)
4. dBins = round(dRange / (c/2) / dt)
   A. This is a 1 by N vector of the number of range bins for each range line we will shift Data_Orig. In other words, this is the elevation compensation for each range line written in terms of range bins.
5. M = M_orig + max(dBins)
6. The original data matrix is zero padded to M and then each range line is shifted by the corresponding entry in dBins.
   A. Because of the round function for creating dBins, the elevation compensation is only done with range bin accuracy.
   B. The new Data matrix is similar to what would have been collected if the aircraft had flown at a constant elevation of maxElev.

7. The elevation matrix is modified according to the elevation compensation so that: Elevation_Orig = Elevation − dBins*dt*c/2. Once again, because of the round function, the Elevation vector will be nearly constant, but not quite; the quantization noise caused by the round function remains.

8. The Time_Orig vector is extended in length by the maximum bin shift to create the new Time vector.

### 2.3.9 Version History

Version 1.1. On June 10, 2011, all of the 2009 Greenland binary files were replaced. The GPS time written in the headers of the previously published binary files contained an error. The error is corrected in the replacement binary files.

Version 1.2. On July 19, 2011, the following changes were made to files in the 2009 Greenland file directory folder /IRSNO1B_SnowRadarXyEcho_v01/2009_GR_NASA/04022009/: Files data00.0005 thru data00.0020 were replaced. Files data00.0001 through data00.0004 were removed, as the recording on the radar froze.

Version 1.3. On 10 February, 2016, all 2009 to 2012 Greenland data were removed from Version 1 IRSNO1B. These data have been converted to netCDF format and added to the Version 2 IRSNO1B data.

### 2.3.10 Error Sources

The CReSIS accumulation, snow, and ku-band data acquisition systems have a known issue with radar data synchronization with GPS time. When the radar system is initially turned on, the radar system acquires UTC time from the GPS National Marine Electronics Association (NMEA) string. If this is done too soon after the GPS receiver has been turned on, the NMEA string sometimes returns GPS time rather than UTC time. GPS time is 15 seconds ahead of UTC time during this field season. The corrections for the whole day must include the offset (-15 second correction). GPS corrections have been applied to all of the data using a comparison between the accumulation, snow, and ku-band radars which have independent GPS receivers. A comparison to geographic features and between ocean surface radar return and GPS elevation is also made to ensure GPS synchronization. GPS time corrections are given in the vector worksheet of the parameter spreadsheet.

## 2.4 Instrumentation

### 2.4.1 Information

As described on the CReSIS Sensors Development Radar Web site, the ultra-wideband radar operates over the frequency range from 2 to 8 GHz to map near-surface internal layers in polar firn with fine vertical resolution. The radar also has been used to measure thickness of snow over sea ice. Information about snow thickness is essential to estimate sea ice thickness from ice freeboard measurements performed with satellite radar and laser altimeters. This radar has been successfully flown on NASA P-3 and DC-8 aircraft.

# 3 SOFTWARE AND TOOLS

MATLAB files may be opened using the NSIDC MATLAB reader, or the Octave high-level language.

JPEG files may be opened using any image viewing program that recognizes the JPEG file format.

KML files are read by GIS software packages and earth browsers such as Google Earth or Google Maps.

# 4 RELATED DATA SETS

IceBridge Accumulation Radar L1B Geolocated Radar Echo Strength Profiles
IceBridge Ku-Band Radar L1B Geolocated Radar Echo Strength Profiles
IceBridge MCoRDS L1B Geolocated Radar Echo Strength Profiles

# 5 RELATED WEBSITES

CReSIS Sensors Development Radar website
CReSIS website
IceBridge product website
IceBridge website at NASA
ICESat/GLAS website at NASA Wallops Flight Facility
ICESat/GLAS website at NSIDC

# 6 CONTACTS AND ACKNOWLEDGMENTS

**Center for Remote Sensing of Ice Sheets (CReSIS)**
Nichols Hall, The University of Kansas
2335 Irving Hill Road
Lawrence, Kansas 66045
data@cresis.ku.edu

# 7    REFERENCES

Carrara, W. G., R. S. Goodman, and R. M. Majewski. 1995. Spotlight Synthetic Aperture Radar: Signal Processing Algorithms, Artech House, Norwood, MA, pp. 26-31.

Kanagaratnam, P., T. Markus, V. Lytle, B. Heavey, P. Jansen, G. Prescott, P. Gogineni. 2007. Ultrawideband Radar Measurements of Thickness of Snow Over Sea Ice, IEEE Transactions on Geoscience and Remote Sensing, 45(9): 2715-2724.

Panzer, B., C. Leuschen, A. Patel, T. Markus, and P. S. Gogineni. 2010. Ultra-wideband Radar Measurements of Snow Thickness Over Sea Ice, Geoscience and Remote Sensing Symposium (IGARSS), 2010 IEEE International, 3130-3133, 25-30 July 2010, doi: 10.1109/IGARSS.2010.5654342.

Panzer, B., C. Leuschen, W. Blake, R. Crowe, A. Patel, P. S. Gogineni, and T. Markus. 2010. Wideband Radar for Airborne Measurements of Snow Thickness on Sea Ice, Abstract C21D-01, 2010 Fall Meeting, AGU, San Francisco, California, 13-17 Dec, 2010.

Kwok, R., C. Leuschen, B. Panzer, A. Patel, N. T. Kurtz, T. Markus, B. Holt, and P. S. Gogineni. 2010. Radar Surveys of Snow Depth Over Arctic Sea Ice During Operation IceBridge, Abstract C21D-02, 2010 Fall Meeting, AGU, San Francisco, California, 13-17 Dec, 2010.

Rodriguez-Morales, F., P. Gogineni, C. Leuschen, C. T. Allen, C. Lewis, A. Patel, L. Shi, W. Blake, B. Panzer, K. Byers, R. Crowe, L. Smith, and C. Gifford. 2010. Development of a Multi-Frequency Airborne Radar Instrumentation Package for Ice Sheet Mapping and Imaging, Proc. 2010 IEEE Int. Microwave Symp., Anaheim, CA, May 2010, 157-160.

Warren, S., I. Rigor, and N. Untersteiner. 1999. Snow Depth on Arctic Sea Ice, Journal of Climate, 12: 1814-1829.

# 8 DOCUMENT INFORMATION

## 8.1 Publication Date

27 March 2013

## 8.2 Date Last Updated

04 October 2018